Journal of Applied Polymer Science

Preparation, Surface Wetting Properties, and Protein Adsorption Resistance of Well-Defined Amphiphilic Fluorinated Diblock Copolymers

Xiaoli Zhan, Guangfa Zhang, Qinghua Zhang, Fengqiu Chen
Department of Chemical and Biological Engineering, Zhejiang University, Hangzhou, Zhejiang 310027, People's Republic of China
Correspondence to: Q. Zhang (E-mail: qhzhang@zju.edu.cn)

ABSTRACT: Novel well-defined amphiphilic fluorinated diblock copolymers P(PEGMA-*co*-MMA)-*b*-PC_6SMA were synthesized successfully by RAFT polymerization and characterized by FTIR, ^{1}HNMR and GPC. For copolymer coatings, static contact angles, θ, with water ($\theta_{water} \geq 109.5°$) and *n*-hexadecane ($\theta_{hexadecane} \geq 68.9°$) pointed to the simultaneous hydrophobic and lipophobic characteristics of the copolymer surfaces. Dynamic contact angle measurements indirectly demonstrated that copolymer films underwent surface reconstruction upon contact with water, which results in a surface with surface coverage of polar PEG units. Moreover, the distinct nanoscale microphase segregation structures were proved by atomic force microscopy (AFM) images. Finally, using bovine serum albumin (BSA–FITC) as the model protein, copolymers exhibited excellent protein adsorption resistance. It is believed that the combination of surface reorganization and nanometer-scale microphase segregation structure endows the excellent protein resistance for amphiphilic fluorinated copolymers. These results provide deeper insight of the effect of surface reconstruction and microphase segregation on the protein adsorption behaviors, and these amphiphilic fluoropolymers can expect to have potential applications as antifouling coatings in the field of marine and biomedical. © 2014 Wiley Periodicals, Inc. J. Appl. Polym. Sci. **2014**, *131*, 41167.

KEYWORDS: biomedical applications; morphology; proteins; surfaces and interfaces

Received 20 March 2014; accepted 15 June 2014
DOI: 10.1002/app.41167

INTRODUCTION

Biofouling caused by attachment of biomacromolecules or whole organisms in aqueous environments, is a ubiquitous problem that can lead to various adverse events.[1,2] For instance, there are thrombosis, microbial infections, and reduction in the performance of an engineering system like marine ship hulls, water filtration membranes, or food industries, etc.[3–5] Therefore, it is necessary to develop advanced low/nonfouling materials or antifouling polymer surfaces for preventing unwanted accumulation of bioadhesion and protein adsorption at surfaces.[6–8]

In recent years in order to improve the fouling-resistant properties, the modifications in hydrophobic or hydrophilic character for the material surfaces have attracted a lot of attention. In general, a hydrophobic surface with a low surface energy can be obtained using fluorinated copolymers or silicone elastomers due to their nonpolar character.[9] For example, Krishnan et al. designed comblike block copolymers with semifluorinated liquid crystalline sidechains, which showed long-lasting hydrophobic and obvious fouling-release performance to organisms.[10] Even though these hydrophobic surfaces can readily release most macrofouling organisms, they cannot deter initial settlement or colonization.[11] In addition, hydrophilic modification of surfaces using poly(ethylene glycol) (PEG) and zwitterionic polymers were found to be promising candidates.[4,7,12–14] However, it is well-known that most microorganisms as well as proteins are inherently amphiphilic; therefore, they operate by different attachment mechanisms.[15,16] Thus, in order to resist fouling upon prolonged exposure to complex aqueous environments, solely hydrophilic or hydrophobic surfaces are inadequate to some extent. Therefore, there is increasing awareness for engineering amphiphilic materials, which can restructure their surfaces depending on the environment.[17–19]

Amphiphilic copolymers composed of hydrophilic and hydrophobic components, which endow the surface dual nature with a compositional and morphological complexity. It is believed that these amphiphilic surfaces have the potential to make it energetically unfavorable for protein adsorption.[20,21] For example, Wooley et al. found a distinct phase segregation between the fluoropolymer and hydrophilic domains took place in the amphiphilic polymer networks with hyperbranched structure, which results in a higher release of Ulva sporelings compared to PDMS.[22] More recently, Zhao et al. reported copolymer films which were prepared by amphiphilic random copolymers. It is found that these copolymers exhibited better antifouling properties for bovine serum albumin (BSA) and human plasma fibrinogen (HFg) than the corresponding homopolymers.[23]

Among of these amphiphilic polymer systems, amphiphilic block copolymer is particularly popular due to its well-defined structure. As mentioned previously, hydrophilic materials like poly(ethylene glycol)(PEG) and zwitterionic materials have been shown to be excellent protein repellency properties.[4,7,12–14] Moreover, the excellent low surface energies of fluoropolymers can significantly reduce the polar and hydrogen-bonding interactions with the bioadhesives or cause the feasible release of the fouling organisms from the coating surfaces.[24,25] Furthermore, many previous publications indicated that the fluorinated units can effectively facilitate the surface coverage of a high-energy hydrophilic groups (such as PEG), which results in excellent fouling resistance for amphiphilic systems.[26–31] Therefore, the tailor-made amphiphilic fluorinated block copolymers would have surprising performance in resisting the protein adsorption.[32]

In this study, the copolymer films with compositional and morphological heteroge- neities on the nanometer-scale were prepared using novel amphiphilic fluorinated block copolymers P(PEGMA-*co*-MMA)-*b*- PC_6SMA. Our previous work has demonstrated that PC_6SMA with short perfluoroalkyl side chains showing excellent hydrophobicity and low crystallizability.[33] These well-defined block copolymers were prepared by RAFT polymerization. As we all know, it is difficult to obtain the diblock copolymers by polymerization of hydrophilic monomer and hydrophobic fluorinated methacrylate due to their remarkable immiscibility.[34,35] Therefore, the random copolymer of PEGMA and MMA was designed as the first block to ensure the solubility of hydrophilic PEGMA and hydrophobic fluorinated component. As far as we know, there have been no reports about employing this type of amphiphilic fluorinated block copolymers for antifouling application. Besides, in this work, the effects of the dynamics surface wettability and microphase segregation of amphiphilic copolymer films on protein resistant properties were investigated in detail. The results would provide an insight into the relationship between the antifouling performance and the amphiphilic surface with compositional and morphological heterogeneities.

EXPERIMENTAL

Materials

The chemical structures of poly(ethylene glycol) methyl ether methacrylate (PEGMA), methyl methacrylate (MMA), [N-methyl-perfluorohexane-1-sulfonamide] ethyl methacrylate (C_6SMA), and 2-(2-cyanopropyl) dithiobenzoate (CPDB) are shown in Figure 1. Poly(ethylene glycol) methyl ether methacrylate (PEGMA, ~300 g mol^{-1}, Aldrich) and methyl methacrylate (MMA, 99.9%, Aldrich) were filtered through a basic alumina column to remove the radical inhibitor. [*N*-methyl-perfluorohexane-1-sulfonamide] ethyl methacrylate (C_6SMA, purity >95%) was synthesized according to the literature.[33] The RAFT agent, 2-(2-cyanopropyl) dithiobenzoate (CPDB) was synthesized and purified according to literature procedures.[36] 2, 2′-Azobisiso-butyronitrile (AIBN, Aldrich) was recrystallized from ethanol. Diphenyl ether, petroleum ether (60–90°C), diethyl ether and butyl acetate were obtained from Sinopharm Chemical Reagent and used as received. Bovine serum albumin labeled with fluorescein isothiocyanate (BSA–FITC) was purchased from WAKO. The PBS buffer solution was prepared in distilled water, and a pH of about 6.9 at 25°C (ionic strength was about 140 m*M*). *n*-hexadecane and *d*-chloroform ($CDCl_3$, 99.8%) were purchased from Aladdin and used as received. Polystyrene-*b*-poly (ethylene-*co*-butylene)-*b*-polystyrene (SEBS) triblock thermoplastic elastomer (Kraton G1643M) was generously provided by Kraton Polymers.

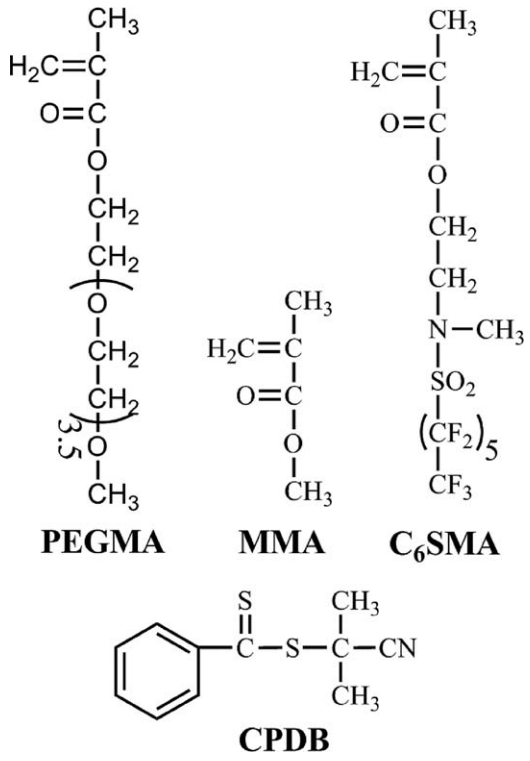

Figure 1. Chemical structures of hydrophilic monomer PEGMA, hydrophobic monomer MMA, hydrophobic/lipophobic monomer C_6SMA, and RAFT agent CPDB.

Polymer Synthesis

A series of amphiphilic fluorinated block copolymers P(PEGMA-*co*-MMA)-*b*-PC_6SMA were prepared by RAFT polymerization.[37] The synthetic procedure was illustrated in Scheme 1. In a typical polymerization, PEGMA, MMA, RAFT agent CPDB, initiator AIBN, and diphenyl ether were added into a flask (50 mL) equipped with a mechanical stirrer, and a reflux condenser. Before the reaction started, the flask was purged with nitrogen for 30 min in order to remove the oxygen, then placed the flask in a constant temperature oil bath at 70°C and reacted for 3–4 h. Polymerization was carried out under a nitrogen atmosphere and was stopped by the cooling of the solutions in an ice bath. The crude product was precipitated in the petroleum ether (60−90°C) for three times, and the random copolymer P(PEGMA-*co*-MMA) was obtained after being dried in vacuum oven at 40°C for 24 h. The recipes of polymerization were summarized in Table I.

Subsequently, P(PEGMA-*co*-MMA)-*b*-PC_6SMA diblock copolymers were synthesized by chain extension of P(PEGMA-*co*-MMA) macro-CTA with C_6SMA (Table II). Macro chain transfer agent P(PEGMA-*co*-MMA), fluorinated monomer C_6SMA

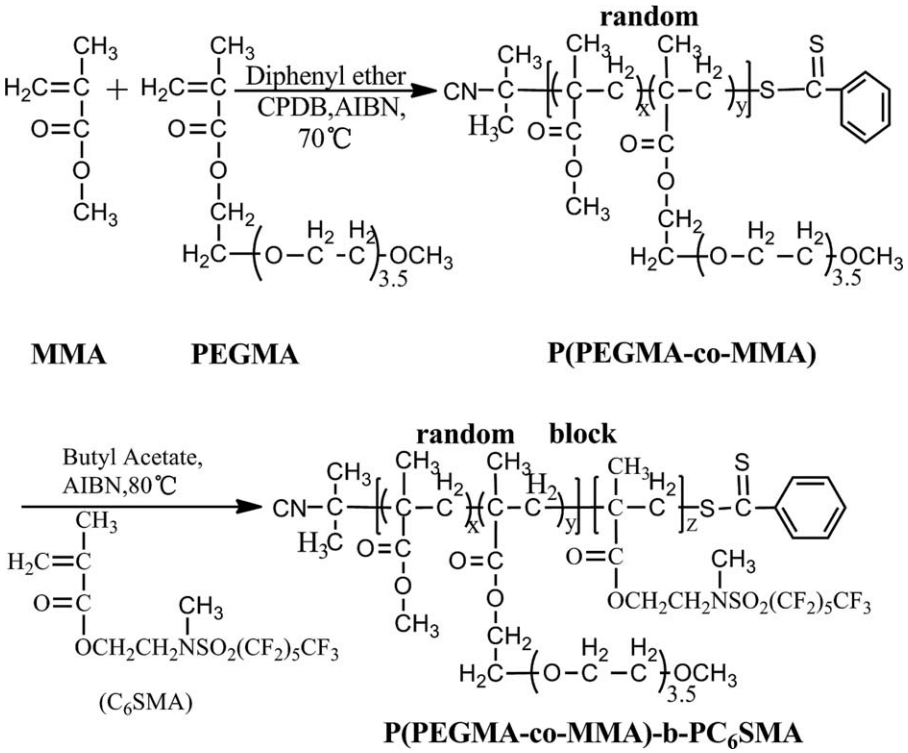

Scheme 1. Synthesis of amphiphilic fluorinated diblock copolymer (PEGMA-*co*-MMA)-*b*-PC_6SMA via RAFT polymerization.

and initiator AIBN were dissolved in butyl acetate, degassed by bubbling nitrogen for 30 min, then placed the flask in a constant temperature oil bath at 80°C and reacted for 24 h. The reaction was stopped by the cooling of the solution in an ice bath. The crude product was precipitated in the diethyl ether. Finally the amphiphilic fluorinated block copolymer P(PEGMA-*co*-MMA)-*b*-PC_6SMA was obtained after being dried in oven at 80°C for 24 h.

Characterization

Fourier transforms infrared spectroscopy (FTIR) and ^{1}HNMR measurements were used to identify the prepared amphiphilic fluorinated block copolymers. GPC analysis was conducted to determine the molecular weight (M_n) and polydispersity index of random copolymers and diblock copolymers prepared by RAFT polymerization. Contact angle measurements, X-ray photoelectron spectroscopy, AFM imaging and BSA protein adsorption testing were employed to determine the surface wettability properties and composition, morphological features, and protein adsorption resistance of amphiphilic fluorinated copolymers.

Copolymers Film Preparation

Copolymers film for contact angle measurements, X-ray photoelectron spectroscopy, AFM imaging, and BSA protein adsorption testing were prepared on silicon wafers/ glass slides by spin-coating 1% (w/v) solutions of P(PEGMA-*co*-MMA)-*b*-PC_6SMA in THF at 2500 rpm using a Cee model 100CB spin coater. These samples were allowed to evaporate at room temperature for 2h in order to remove the solvent. SEBS control surface was prepared in an analogous fashion using THF as solvent. All coatings were annealed in a vacuum oven at reduced pressure at 130°C for at least 12 h followed by slow cooling to room temperature.

FTIR, ^{1}HNMR, and GPC analysis

FTIR spectra of the block copolymers cast as films from THF solution on KBr disks (KBr crystal plates) were collected using a Nicolet 5700 FTIR instrument. ^{1}HNMR (vs TMS) spectra of the block copolymers were recorded using a Bruker 500MHz nuclear magnetic resonance spectrometer (Advance DMX500) and were carried out with a 5 wt % solution in $CDCl_3$ at room temperature. The number average molecular weight and polydispersity index of copolymers were measured by Waters 1525/ 2414 gel permeation chromatography (GPC) system consisting of a Waters 1525 binary high-performance liquid chromatography pump, a Waters 717 plus auto-sampler, three Waters Styragel columns (Styragel HR_2, HR_3, and HR_4), and a Waters 2414 refractive index detector. THF was used as the eluent at a flow rate of 1.0 mL min^{-1} at 35°C. Polystyrene standards [$(4.0 \times 10^2) - (4.0 \times 10^5)$ g/mol] were used for calibration.

Contact Angle Measurements

The static and dynamic contact angles were measured by a CAM200 optical contact angle meter (KSV Co., Ltd.) at room temperature. The static contact angles of water and *n*-hexadecane were measured on SEBS control and block copolymer surfaces using the sessile drop technique. The surface tension of the copolymer films was calculated from the static contact angles referring to the so-called Owens-Wendt-Kaelble approach.[38,39] The dynamic contact angles were measured using an inclinable plane.[33] On an inclinable plane, a sample on a stage was tilted until a 50 μL water droplet began to slide down

Table I. Recipe for Random Polymerization of PEGMA and MMA at 70°C

		PEGMA/MMA wt/wt[a]				
Ingredient	Material	Expt1 20/80	Expt2 40/60	Expt3 50/50	Expt4 60/40	Expt5 80/20
monomer	PEGMA	4.0 g	8.0 g	10.0 g	12.0 g	16.0 g
	MMA	16.0 g	12.0 g	10.0 g	8.0 g	4.0 g
RAFT agent	CPDB	0.688 g	0.688 g	0.688 g	0.688 g	0.688 g
solvent	diphenyl ether	46.67 g	46.67 g	46.67 g	46.67 g	46.67 g
initiator	AIBN	0.102 g	0.102 g	0.102 g	0.102 g	0.102 g

[a] The weight ratio of PEGMA and MMA monomers in feed.

onto the sample. Subsequently, an advancing contact angle (θ_a), a receding contact angle (θ_r), and contact angle of hysteresis ($\theta_{h,}=\theta_a-\theta_r$) were determined.

XPS Analysis

X-ray photoelectron spectroscopy (XPS) spectra were recorded with a VG ESCALAB MARK II spectrometer with a standard Mg Kα X-ray source (1253.6 eV) operating at 300 W. The working pressure was less than 10^{-7} Pa. Extended spectra (survey) were collected in the range 0–1060 eV (50 eV pass energy). Detailed spectra were recorded for the following regions: C(1s), O(1s), and F(1s) (50 eV pass energy). The standard deviation in the BE values of the XPS line was 0.10 eV. To take into account charging problems, the C(1s) peak was considered at 284.8 eV and the peak BE differences were evaluated.

AFM Imaging

AFM experiments were performed with a Nanoscope III scanning probe microscope from Digital Instruments. The surface morphologies and topographies were investigated in the tapping mode with a Digital Instruments Bioscope instrument (dimension head and G scanner) under ambient conditions, with a silicon tip (160 μm, 325 kHz) with a nominal spring constant of 40 N/m.

BSA Protein Adsorption Testing

Totally, 50 μL of bovine serum albumin (BSA) labelled with fluorescein isothiocyanate (BSA–FITC) solution in PBS was diluted in 10 mL of PBS solution, and the concentration of the resulting solution was 0.05 mg/mL. Amphiphilic fluorinated block copolymers were spun-coat on silicon wafers. Additionally, an uncoated silicon wafer, cleaned for 2 min with a Harrick PDC-32G oxygen plasma cleaner, was used as a control. These silicon wafers were then incubated in BSA–FITC solution in a dark room for 1 h and rinsed with deionized water thoroughly afterwards. Fluorescence microscopy was performed using an Olympus BX61W1-FV1000 upright microscope with a 40 × UPlan Fluorite 40 × dry objective (NA 0.75). Images were acquired using a Roper CoolSnap HQ CCD camera and Image Pro image acquisition and processing software. Fluorescein and FITC were observed with a 450 nm excitation and 550 nm emission filter set.

RESULTS AND DISCUSSION

Polymer Synthesis and Characterization

In this work, a series of amphiphilic fluorinated block copolymers P(PEGMA-*co*-MMA)-*b*-PC_6SMA with different hydrophilic PEGMA and fluorinated PC_6SMA compositions were prepared by RAFT polymerization. A two-step synthesis was used to prepare these copolymers. In the first step, random copolymer P(PEGMA-*co*-MMA) was synthesized with CPDB as the chain transfer agent, since CPDB has recently been successfully used in the RAFT polymerization of methacrylate.[40,41] Subsequently, P(PEGMA-*co*-MMA)-*b*-PC_6SMA) diblock copolymer was synthesized by chain extension of P(PEGMA-*co*-MMA) macro-CTA with C_6SMA.

The results of GPC analyses of P(PEGMA-*co*-MMA) Macro-CTA and the corresponding P(PEGMA-*co*-MMA)-*b*-PC_6SMA copolymers are shown in Table III and Figure 2. In comparison with P(PEGMA-*co*-MMA) Macro-CTA, the molecular weight of block copolymers have a significant increase and still remain relatively low polydispersity index (PDI<1.26). These results clearly suggest that a successful chain extension producing well-defined amphiphilic fluorinated P(PEGMA-*co*-MMA)-*b*-PC_6SMA copolymers. The solution of block copolymers in THF foamed strongly upon shaking, which confirmed indirectly the formation of fluorinated copolymers.[42]

The chemical composition of block copolymers can be identified by ^{1}H NMR and FTIR spectra. Figure 3(a) shows the ^{1}HNMR spectra of P(PEGMA-*co*-MMA)-*b*-PC_6SMA copolymers(A, B, D, and E), and the characteristic peaks and relative chemical shift are very similar. The characteristic peaks of P(PEGMA-*co*-MMA) block can be clearly seen at ~3.38ppm (Peak c) and

Table II. Recipe for Synthesis of Block Copolymers P(PEGMA-*co*-MMA)-*b*-PC_6SMA

Ingredient	Material	Expt1	Expt2	Expt3	Expt4	Expt5
macro-CTA	P(PEGMA-*co*-MMA)	2.0 g	1.5g	1.0 g	1.5 g	2.0 g
monomer	C_6SMA	3.33 g	2.367 g	1.621 g	2.046 g	2.93 g
initiator	AIBN	0.011 g	0.008 g	0.005 g	0.007 g	0.010 g
solvent	Butyl acetate	15.99 g	11.601 g	7.861 g	10.638 g	14.79 g

Table III. The GPC Results of Random Copolymers and Block Copolymers

	P(PEGMA-*co*-MMA)				P(PEGMA-*co*-MMA)-*b*-PC_6SMA		
Expt	PEGMA wt %		M_n (g/mol)[c]	PDI	Copolymer sample[d]	M_n (g/mol)[c]	PDI
	Feed[a]	Copolymer[b]					
1	20	18.9	5997	1.26	A	9750	1.24
2	40	38.9	6277	1.22	B	8200	1.15
3	50	48.2	6171	1.26	C	8158	1.17
4	60	56.0	7138	1.22	D	11804	1.23
5	80	72.0	6638	1.25	E	9535	1.22

[a] The weight fraction of PEGMA in feed materials.
[b] Calculated from the characteristic proton integrals of ^{1}HNMR spectra.
[c] Against polystyrene standards.
[d] Block copolymers with different compositions.

∼ (3.55–3.66)ppm (Peak b) due to protons of methoxy (—OCH_3) and methylene (—OCH_2CH_2—), respectively. Additionally, signals at ∼4.1 ppm (Peak a) are assigned to -CH_2 protons of the PEG side chain in P(PEGMA-*co*-MMA) block next to —OC═O. Signals d at ∼3.17 ppm originate from the —CH_3 protons of -NCH_3 in PC_6SMA block. The signals at ∼(0.84–2.03) ppm (Peak e) are assigned to the backbone (—CH_2—) and —CH_3 protons of methacrylate in P(PEGMA-*co*-MMA)-*b*-PC_6SMA).

^{1}HNMR (400MHz, $CDCl_3$, δ/ppm) : A : δ4.09 (s, a,-OCH_2-), δ3.55–3.66 (m, b, -OCH_2CH_2-), δ3.38 (s, c, -OCH_3), δ3.17 (s, d, -NCH_3), δ0.85-2.03 (m, e, C-CHX); B : δ4.10 (s, a,-OCH_2-), δ3.59–3.66 (m, b, -OCH_2CH_2-), δ3.38 (s, c, -OCH_3), δ3.17(s, d, -NCH_3), δ0.84-2.03(m, e, C-CHX); D : δ4.10 (s, a,-OCH_2-), δ3.60–3.66(m, b, -OCH_2CH_2-), δ3.38(s, c, -OCH_3), δ3.16 (s, d, -NCH_3), δ0.84-2.04 (m, e, C-CHX); E : δ4.10(s, a,-OCH_2-), δ3.56–3.66 (m, b, -OCH_2CH_2-), δ3.38 (s, c, -OCH_3), δ3.16 (s, d, -NCH_3), δ 0.85–2.03 (m, e, C-CHX).

The FTIR spectra of P(PEGMA-*co*-MMA) -*b*-PC_6SMA) diblock copolymers(A, B, D, and E) are shown in Fig. 4(a). As seen from the Fig. 4(a), the characteristic absorptions of C=O (1731cm^{-1}), aliphatic C-H stretch (2850∼ 2960cm^{-1}), and C-F stretch (1147.9∼ 1239.2 cm^{-1}) are clearly visible. Meanwhile, the characteristic stretching of double bond at frequencies of 1630 cm^{-1} disappeared. This confirms that the monomers have been polymerized. Fig. 4b shows the FTIR spectra of random copolymer P(PEGMA-*co* -MMA), C_6SMA, and corresponding diblock copolymer (D). The spectrum of diblock copolymer include the characteristic peaks of P(PEGMA-*co*-MMA) and C_6SMA. Thus, the formation of fluorinated diblock copolymers by RAFT solution polymerization was confirmed by ^{1}HNMR and FTIR characterization.

Surface Wettability and Surface-Free Energy

The fouling resistance performance of copolymer films is strongly dependent on its surface properties, such as wettability, morphology, and interfacial characteristics. Therefore, prior to protein adsorption studies, detailed surface characterization was performed. To explore the wettability and surface energy of amphiphilic copolymer films, the static and dynamic contact angles of water and *n*-hexadecane on the copolymer surfaces and the SEBS control were measured using the sessile drop technique.[29] Additionally, The measured values of dynamic contact angles (θ_a, θ_r and average contact angle $\overline{\theta}$) were then used

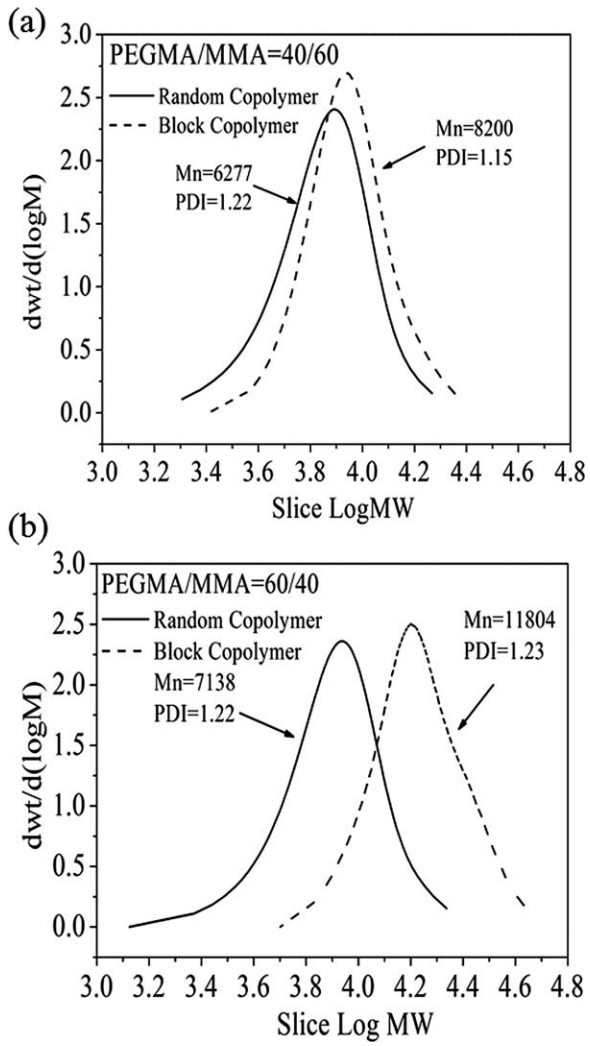

Figure 2. GPC traces of P(PEGMA-*co*-MMA) Macro-CTA and P(PEGMA-*co*-MMA)-*b*- PC_6SMA block copolymers in THF, (a) and(b) represent Experiments 2 and 4, respectively.

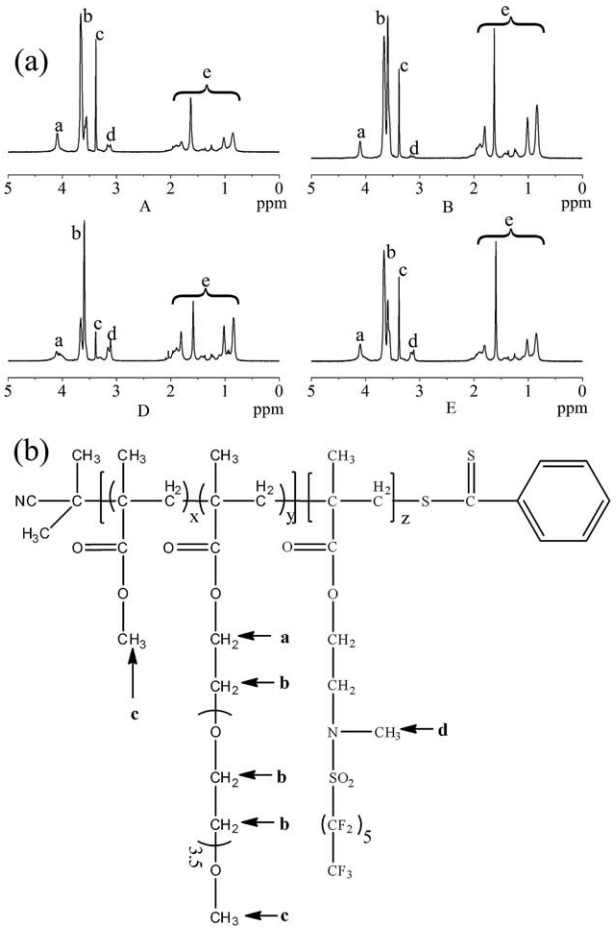

Figure 3. (a) ^{1}HNMR spectra of amphiphilic fluorinated diblock copolymers in $CDCl_3$, A, B, D, and E are shown in Table III. (b) The protons type of diblock copolymers.

to extract the surface tension of the polymer films referring to the Owens-Wendt-Kaelble approach.[38] According to Fowkes,[43] the surface tension (γ) can be resolved into a dispersion component (γ^d) and a polar component (γ^p) [eq. (1)].

$$\gamma=\gamma^d+\gamma^p \tag{1}$$

Where γ is the total surface tension, γ^d is the dispersion component, and γ^p is the polar component. The total surface-free energies of the coatings were computed as the sum of the γ^d and γ^p terms.

Owens et al.[38]extended this concept and proposed the following semiempirical equation:

$$\gamma_L(1+\cos\theta)=2\left(\gamma_s^d\gamma_L^d\right)^{1/2}+2\left(\gamma_s^p\gamma_L^p\right)^{1/2} \tag{2}$$

In eq. (2), subscript "L", "S" refers to the wetting test liquid and the solid, respectively, and θ is the contact angle. The surface tension of the solid surface γ_s, γ_s^d, and γ_s^p can be determined by eq. (2) and two different liquids whose surface tension (γ_L), dispersion (γ_L^d), and polar components (γ_L^p) are known. Water ($\gamma_L^d=21.8$ m*N*/m; $\gamma_L^p=51.0$ m*N*/m) and hexadecane ($\gamma_L^d=27.5$ m*N*/m; $\gamma_L^p=0$ m*N*/m) were used in this work as the test liquids to measure the surface tension. The contact angles of water and hexadecane measured for block copolymers (A, B, C, D, and E) are shown in Table IV.

As seen in Table IV, the SEBS control surface shows both hydrophobic and lipophilic characteristics. However, the amphiphilic fluorinated copolymers (A–E) turned out to be both excellent hydrophobic and lipophobic character at the same time, being $\theta_{water}\geq 109.5^\circ$ and $\theta_{hexadecane}\geq 68.9^\circ$ (static contact angles in Table IV). This is due to the low surface energy fluorinated segments migrated to the polymer-air interface after annealing treatment. The dynamic contact angles (advancing and receding contact angles, θ_a and θ_r) for copolymers and SEBS control are also given in Table IV. For the surface of homopolymer, the static contact angle θ_s is commonly used for surface calculations, however, for amphiphilic surfaces, the receding contact angle (θ_r) or the average contact angle ($\overline{\theta}$, $\cos\overline{\theta}=(\cos\theta_a+\cos\theta_r)/2$) are probably more reasonable for estimating the surface energy parameters.[44]

In this work, the surface tensions γ_S calculated with all three angles θ_a, θ_r, and $\overline{\theta}$ are presented in Table V. Additionally, the surface energy of the SEBS was also estimated for comparison. In general, the values of surface energy would be influenced by the surface concentrations of the polar (PEG segments,

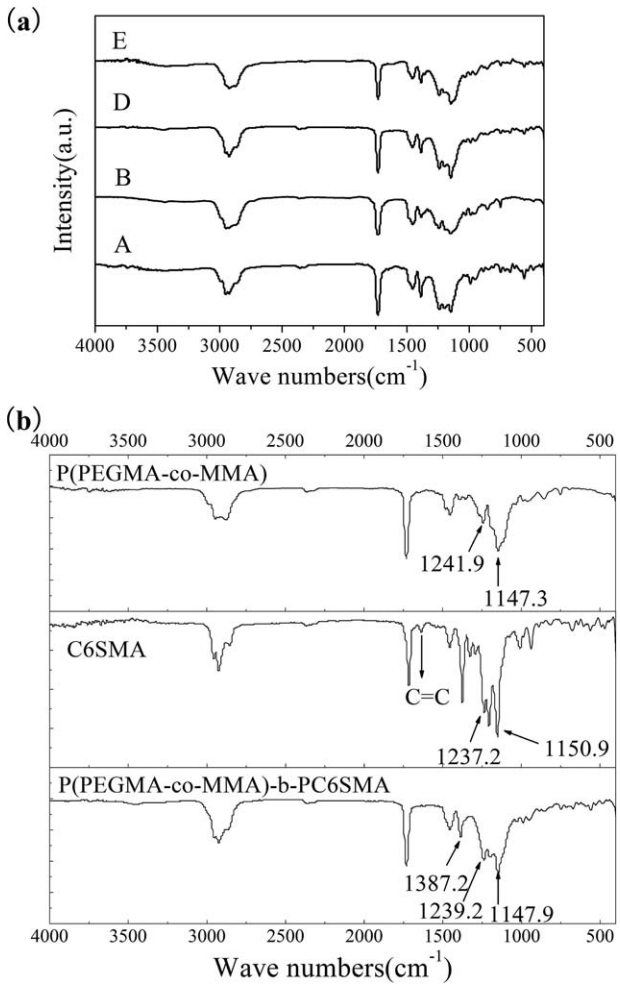

Figure 4. (a) The FTIR spectra of amphiphilic fluorinated diblock copolymers, (A, B, D, and E are shown in Table III). (b) The FTIR spectra comparison of P(PEGMA-*co*-MMA) (Expt 4), C_6SMA, and corresponding diblock copolymer (D).

Table IV. θ_s, θ_a, and θ_r (°) Values of Different Probe Liquids on the Surfaces of the Amphiphilic Fluorinated Block Copolymers and the SEBS Control

Sample	PC_6SMA[a] (wt %)	P(PEGMA)[b] (wt %)	WA[c]				HD[c]		
			θ_S[a]	θ_a[a]	θ_r[a]	θ_h[a]	θ_s	θ_a	θ_r
SEBS[d]			110.3	115.2	103.5	11.7	38.1	39.3	26.3
A	38.5	12.3	114.1	122.1	110.6	11.5	73.7	72.6	62.7
B	23.5	30.6	109.5	110.0	85.0	25.0	68.9	70.3	60.3
C	24.4	37.8	114.5	116.5	94.4	22.1	73.3	72.4	61.8
D	39.5	36.3	112.0	115.8	90.0	25.8	71.4	72.5	63.4
E	30.4	55.7	113.1	113.2	88.2	25.0	71.1	72.0	63.5

θ_s, static contact angle; θ_a, advancing contact angle; θ_r, receding contact angle; θ_h, the water contact angle hysteresis.
[a] The weight fraction of PC_6SMA block in block copolymer.
[b] The weight fraction of PEGMA component in block copolymer.
[c] WA, water; HD, hexadecane.
[d] The control surface.

hydroxyl, amide, and ester groups, etc.) and nonpolar groups (such as perfluoroalkyl segments, etc.)[26] As seen from Table V, the total surface energies of amphiphilic copolymers, determined with the θ_a values, were remarkably lower than that of the SEBS control and polytetra fluoroethylene (PTFE) (18 mJ/m^2).[31,33] Previous publication proved that the fluoroalkyl segments can effectively lower the surface energy, even when small numbers of the groups were fluorinated.[24] Hence, the relatively low surface energy, calculated with θ_a, was attributed to the fluoroalkyl segments enriched on the outmost surface. The θ_a values were mainly influenced by the highly nonpolar perfluoroalkyl groups in the amphiphilic fluorinated copolymers.

On the other hand, the surface energy parameters calculated with θ_r are also shown in the Table V. It is evident that the total surface energy values are higher than that determined with the θ_a values. However, the hydrophobic SEBS homopolymer had nearly the same surface energy, regardless of whether θ_a or θ_r was used for the surface energy calculation. Thus, for the surfaces of the amphiphilic copolymers consisting of both polar and nonpolar groups, θ_a was influenced primarily by the nonpolar segments (such as the perfluoroalkyl groups), whereas θ_r was determined with the polar groups (PEG segments, etc.) at the surface. For homopolymer surfaces, which only have one polarity, both the contact angles resulted in similar values of surface energy.

Surface Reorganization

The advancing and receding contact angles of water, summarized in Table IV, upon the SEBS control and the amphiphilic copolymer films were determined using an inclinable plane.[33] The advancing contact angles (θ_a) of water on the copolymer films and the SEBS control were similar to those of static contact angles, which were affected by the composition of fluorinated components and hydrophilic PEG segments in these copolymers. The receding contact angles (θ_r) of water, summarized in Table IV, reflected slightly hysteresis of contact angle ($\theta_h = \theta_a - \theta_r$) upon all of the amphiphilic fluorinated copolymer films (A-E). The water contact angle hystereses were 11.5, 25.0, 22.1, 25.8, and 25.0, for the copolymer surfaces with PEG wt % of 12.3, 30.6, 37.8, 36.3, and 55.7%, respectively. In general, contact angle hysteresis is caused by factors such as surface roughness, chemical heterogeneity, and surface reconstruction of the copolymer films after contact with the aqueous environment.[16, 21, 22, 45] In the present work, the investigated amphiphilic copolymer films showed a fairly low AFM roughness (Root Mean Square, rms $\sim$ 1nm) and its effect on hysteresis would be negligible. Therefore, the experimentally observed values of θ_h are most likely due to a combination of surface compositional heterogeneity and surface reconstruction.[21]

In the present work, the hydrophilic segments PEG possess low polymer–water interfacial energy and the hydrophobic segments PC_6SMA just possess low crystallinity.[33] Therefore, these

Table V. Surface Energies (mJ/m^2) of the Amphiphilic Fluorinated Block Copolymers and the SEBS Control Calculated with OWK Model

Sample	γ_s^d			γ_s^p			γ_s		
	With θ_a	*With* θ_r	*With* $\overline{\theta}$	*With* θ_a	*With* θ_r	*With* $\overline{\theta}$	*With* θ_a	*With* θ_r	*With* $\overline{\theta}$
SEBS	21.6	24.7	23.2	0.0	0.4	0.1	21.6	25.1	23.3
A	11.6	14.6	13.1	0.0	0.6	0.2	11.6	15.2	13.3
B	12.3	15.4	13.8	1.1	8.9	4.1	13.4	24.3	17.9
C	11.7	14.9	13.2	0.3	4.8	1.9	12.0	19.7	15.1
D	11.6	14.4	13.0	0.4	6.8	2.7	12.0	21.2	15.7
E	11.8	14.4	13.0	0.7	7.7	3.3	12.5	22.1	16.3

[a] $\overline{\theta}$, average angle calculated with $\cos\overline{\theta} = (\cos\theta_a + \cos\theta_r)/2$.

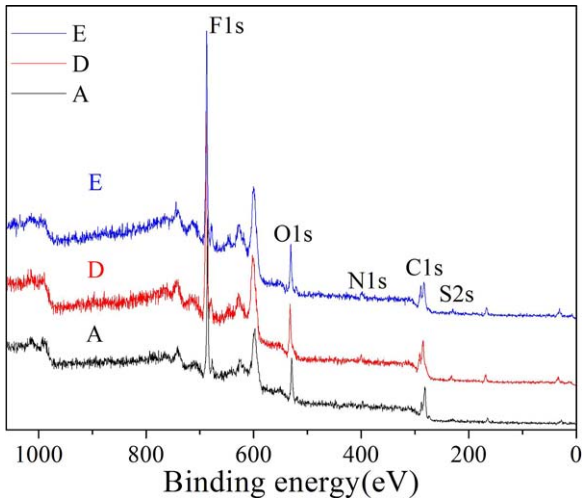

Figure 5. XPS survey spectra for block copolymers A, D, and E (Table III). [Color figure can be viewed in the online issue, which is available at wileyonlinelibrary.com.]

amphiphilic copolymers would have responsive ability for the wetting environment. In the dry state, because of the low surface energy, the fluorinated segments would readily migrate to the polymer-air interface and being enriched at the interface. However, once the copolymer surfaces contacting with water, in order to reduce the interfacial energy, the flexible PEG chains would stretch out and the fluorinated segments tended to be segregated in the bulk of the film. As a result of the surface reconstruction, the copolymer surfaces became more enriched in the hydrophilic PEG units. Martinelli et al. have observed similar behaviors for polystyrene block copolymers carrying an amphiphilic polyoxyethylene-polytetra-fluoroethylene chain side group.[21] In brief, The contact angle hysteresis of these copolymer films was mainly caused by the surface reconstruction, which may be have a great influence to the protein adsorption resistance behavior.

XPS Analysis

The quantitative analysis of the surfaces composition was performed by X-ray photoelectron spectroscopy (XPS) measurements on the copolymers films. As seen in Figure 5, the survey spectrum of block copolymers showed the signals due to the elements constituting the repeat units: C(~290eV), O(~532eV), F(~688eV), N, and S. The results agree with the chemical composition of amphiphilic fluorinated block copolymers P(PEGMA-*co*-MMA)-*b*-PC_6SMA. Furthermore, Figure 6 shows a high-resolution XPS spectrum of C(1s) of the block copolymer D. The C(1s) of the block copolymer D could be resolved into five peaks at binding energies of 284.2, 285.5, 287.9, 291.0, and 293.4 eV, which were attributed to C—C, C—O(C—N, and C—S), C═O, CF_2, and CF_3, respectively.

The atomic composition data for the surfaces and the corresponding values calculated from the known stoichiometric ratios of block copolymers are summarized in Table VI. For all of the three block copolymers, the high-resolution XPS spectrum of F(1s), C (1s), and O(1s) and were also determined. The block copolymer A was used as a typical example, the atomic composition data showed in the Table VI were calculated from the following method. First, the area of high-resolution XPS spectrum of F(1s), C(1s), and O(1s) were integrated separately, and the results were 9593.0, 3142.0, and 2493.5, respectively. After that, these areas were divided by corresponding sensitivity factors (1.000, 0.278, and 0.780, respectively), and then the atomic compositions of F, C, and O for block copolymer A were calculated for 39.8%, 46.9%, and 13.3%, respectively. It was found that the elemental composition of the copolymer samples had a significant difference between the outer surface and theoretical values calculated from the known composition after annealing at 130°C for 20 h. Take block copolymer D for example, the surface content of F was significantly higher than that of theoretical value, e.g., decreased from 35.9% to 15.5%, while the C, O percentage followed the opposite trend, increasing from 50.6%, 13.5% to 60.3%, 24.2%, respectively. Furthermore, the experimental F/C ratio (0.71) was much higher than the theoretical one (0.26). Meanwhile, the atomic composition of block copolymers A and E had the same trend as those of the block copolymer D.

These findings demonstrated that the outermost surface of amphiphilic block copolymers was enriched in fluorine with

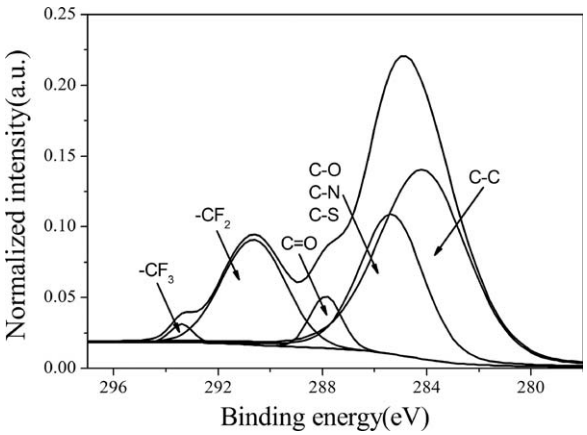

Figure 6. Area-normalized C(1s) XPS signals for block copolymer D after annealing at 130°C.

Table VI. XPS atomic Compositions for Block Copolymers A, D, and E After Annealing at 130°C

		Atomic compositions			
Polymer film		*F* (%)	*C* (%)	*O* (%)	*F/C*
A	Experimental[a]	39.8	46.9	13.3	0.85
	Stoichiometric[b]	15.0	61.3	23.7	0.24
D	Experimental	35.9	50.6	13.5	0.71
	Stoichiometric	15.5	60.3	24.2	0.26
E	Experimental	34.5	49.3	16.2	0.70
	Stoichiometric	11.8	62.1	26.1	0.19

[a] The experimental values were determined based on the XPS measurement.
[b] Calculated on the basis of the known composition of the block copolymers.

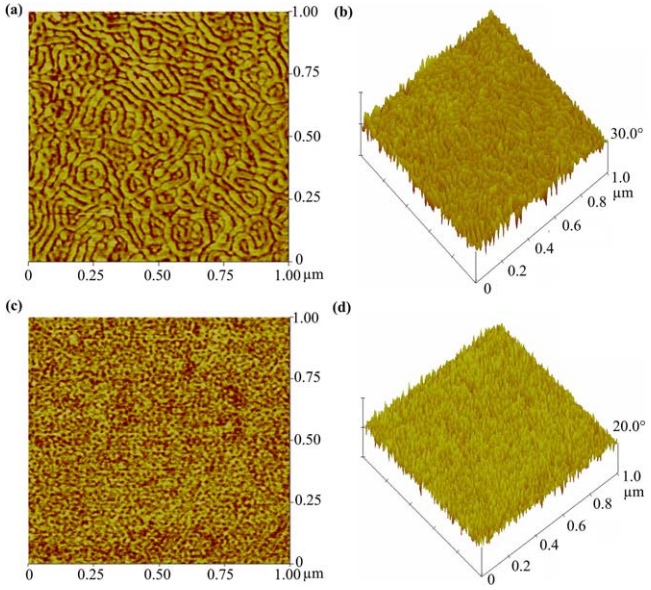

Figure 7. AFM two-dimensional phase image (a), (c), and three-dimensional phase image (b), (d) for block copolymers A and E, respectively, taken in air (tapping mode). [Color figure can be viewed in the online issue, which is available at wileyonlinelibrary.com.]

respect to the bulk,[21] and the enrichment of fluorinated groups can significantly lower surface free energy. In addition, isothermal annealing for block copolymer films promoted enrichment in fluorinated chains at the outermost surface, owing to their low surface free energy. Thus, the XPS results explain the phenomenon that the excellent hydrophobic and lipophobic characteristics of the target block copolymers in the dry state. Many other examples have been reported in the literature about the selective segregation of semifluorinated chains of a polymeric structure at the polymer-air interface.[46,47] However, the fluorinated segments in the block copolymers herein became easier to separate as a consequence of having less constraint by the other segments, which resulted in a much higher content of fluorine at the topmost surface.

Surface Morphology

The block copolymers containing hydrophilic PEG segments and hydrophobic fluorinated segments have significantly different polarities, which would lead to mutual chemical incompatibility. AFM analysis was used in this article to investigate the microphase structure and morphological features of the amphiphilic fluorinated co-polymer films after annealing treatment. For block copolymers A and E, both of the copolymer surfaces exhibited distinct microphase separation structure between hydrophilic PEG and hydrophobic fluorinated domains, which was resulted from the thermodynamically induced phase segregation.[48]

As shown in Figure 7, the dark area in the images represents the soft segments of PEG domain and the bright area demonstrates the aggregation of fluorinated chains with high glass transition temperature and low crystallinity.[33] The AFM images show that the surfaces of the block copolymer films are mainly composed of the bright areas, which further confirms the enrichment of fluorinated groups on the surface. As seen from Fig. 8, the film surfaces of block copolymers A and E exhibit low surface roughness values (Root Mean Square, rms ~ 1nm), which supports the inference presented previously that contact angle hysteresis (θ_h) is most likely due to a combination of surface composition heterogeneity and surface reconstruction. In addition, it is found that the surface roughness is independent of the chemical composition of the amphiphilic block copolymers.

The microphase separation structure indicates that incompatibility of the two segments in the amphiphilic copolymers would lead to self-assembled heterogeneous structure composed of hydrophilic PEG and hydrophobic fluorinated domains. The microphase separation structure depends on the amphiphilic copolymer composition. With the weight ratio of PEGMA/PC_6SMA increasing from 0.32 to 1.55(block copolymers A and E, respectively), the microphase separation structure transfers from lying cylinders to spherical domains. It is also found that the phase separation scale for these samples is in the range of 20–30 nm which is near the common protein scale such as BSA, and thus such nanostructures would play a unique role for protein adsorption resistance.

Fluorescence Microscopy of BSA–FITC Incubated Samples

Protein adsorption behavior of a given material depends mainly on surface free energy and chemical functionality.[49] It is well-known that hydrophobic surfaces have evidenced a tendency to adsorb proteins at elevated levels as hydrophobic effect. However, hydrophilic surfaces such as poly(ethylene glycol) (PEG) and zwitterionic polymers possess excellent resistance to protein adsorption and cellular adhesion.[50, 51] Amphiphilic copolymers

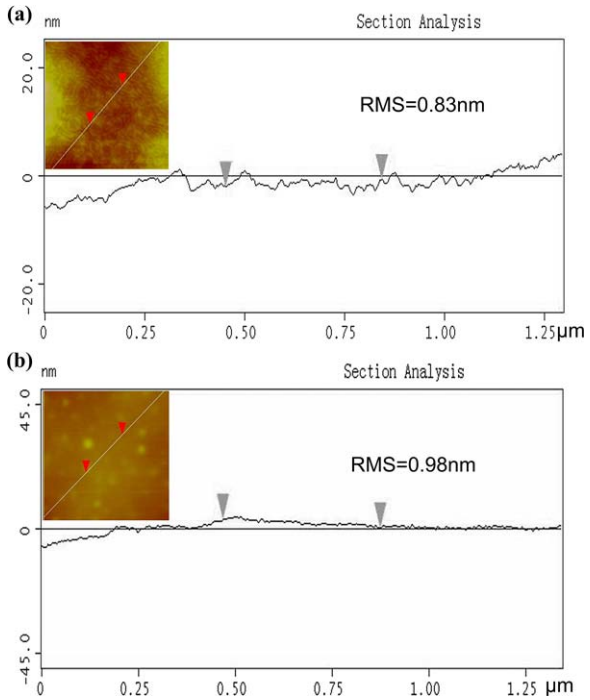

Figure 8. The surface roughness (Root Mean Square) of block copolymer films A (a) and E (b). [Color figure can be viewed in the online issue, which is available at wileyonlinelibrary.com.]

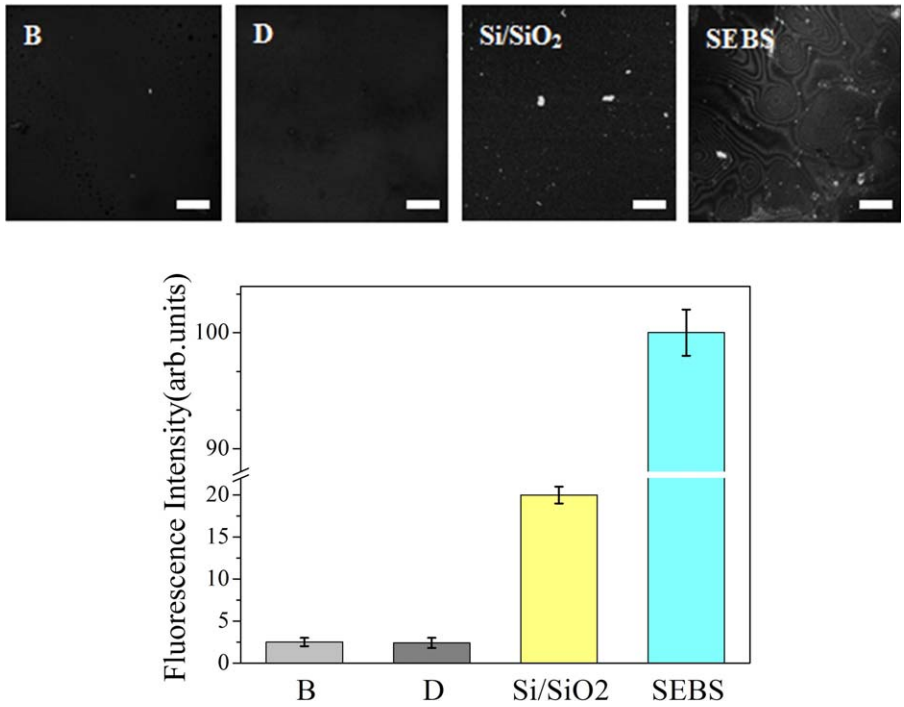

Figure 9. Fluorescence microscopy intensity results of BSA–FITC incubated samples. B and D represent block copolymers B and D, respectively; The bar graph gives the relative fluorescence intensity of the four samples when the SEBS control was normalized to 100. Scar bar: 60 μm. [Color figure can be viewed in the online issue, which is available at wileyonlinelibrary.com.]

contain both hydrophobic and hydrophilic moieties, thus the protein adsorption behavior of the amphiphilic copolymers is of great interest, and is also the focus of our research.

As shown in Figure 9, the amount of adsorbed protein on these amphiphilic copolymer films are significantly less than that on the hydrophilic Si/SiO_2 (silicon wafer) surface and hydrophobic SEBS control surface (the SEBS control was normalized to 100). The findings indicated that the amphiphilic fluorinated block copolymer has excellent protein adsorption resistance properties for bovine serum albumin (BSA). However, considering the surface properties of amphiphilic copolymer discussed previously, i.e., the copolymer surfaces after annealing in the dry state showed a strong hydrophobicity, the finding is surprising. Many previous studies showed that within a given system, as the increase of hydrophobicity of the coating, its ability to resist nonspecific adsorption decreases.[52] In the case of P(PEGMA-*co*-MMA)-*b*-PC_6SMA, which has high hydrophobicity, it is clear that its ability to resist protein adsorption is due to the presence of fluorinated side chains. One likely explanation to the efficacy of copolymers in resisting nonspecific protein adsorption is the increased surface coverage of the PEG functionality, which is aided by the low surface energy of the fluorinated side chains. While this is not directly evident from the wetting experiments performed on copolymers, the hysteresis of the surface indicates surface reorganization. Although the high water contact angle of copolymers is indicative of a large concentration of fluorinated side chains on the surface, they can reorganize when immersed in hydrophilic media (such as water) to expose the PEG functionality on the surface. This results in a surface with high surface coverage of PEG units. Furthermore, as we all know, protein is inherently amphiphilic (both poessess polar and nonpolar components), thus fluorinated functionality could lead to a repulsive effect against both polar and nonpolar (lipophilic) components of the protein.[31] Therefore, both the PEG and fluorinated functionalities on the surface resulted in the excellent protein resistance in this paper.

In fact, bioadhesion is a very complex process, since many factors such as surface chemistry, surface morphology, and surface charge play important roles.[3] Therefore, the surface phase segregation with nanometer-scale pattern would affect the protein adsorption also. While a typical protein has areal dimensions of 10–1000 nm^2, such as BSA is soft and globular with the dimensions of 4 nm $\times$ 4 nm $\times$ 14 nm, the initial areas for end-on and side-on adsorption would be 56 and 16 nm^2, respectively.[53] In this study, the surface phase segregation pattern on nanometer-scale (20–30 nm) near the size scale of BSA is believed potentially disrupt the adsorption event and therefore enhance resistance to protein adsorption.[54] In brief, the combination of surface reorganization exposing the PEG functionality on the surface and nanometer-scale phase segregation structure imparts the excellent protein resistance for amphiphilic fluorinated copolymers.

CONCLUSIONS

In this work, we have designed a novel amphiphilic fluorinated block copolymers composed of hydrophilic, hydrophobic, and fluorinated monomers, and then the adsorption behaviors of BSA-FITC on the copolymer surfaces were investigated. Surprisingly, the amphiphilic fluorinated surfaces exhibited excellent protein resistance compared with the hydrophilic silicon wafer.

Detailed surface characterization showed that the amphiphilic fluorinated block copolymer surface is dynamic to some extent. In the dry state, the fluorinated segments migrated to the polymer-air interface, resulting in a strongly hydrophobic surface. However, when amphiphilic fluorinated block copolymers were immersed in a hydrophilic media such as aqueous environment, the PEG units would readily to expose on the surface. Besides, it was believed that the phase segregation pattern on nanometer-scale (20–30 nm) near the size scale of BSA strongly affected the adsorption behaviors of protein. In brief, the excellent protein adsorption resistance of the amphiphilic coatings was mainly due to the surface reorganization of PEG units and the phase segregation pattern on nanometer-scale (20–30 nm). This study provides an insight into the relationship between the antifouing performance and the corresponding amphiphilic surface with compositional and morphological heterogeneities.

ACKNOWLEDGMENTS

The authors thank for financial supports from the National Natural Science Foundation of China (No.21076184, 21176212) and Zhejiang Provincial Natural Science Foundation of China (LY14B060008).

REFERENCES

1. Werner, C.; Maitz, M. F.; Sperling, C. *J. Mater. Chem.* **2007**, *17*, 3376.
2. Martinelli, E.; Sarvothaman, M. K.; Alderighi, M.; Galli, G.; Mielczarski, E.; Mielczarski, J. A. *J. Polym. Sci. Part A: Polym. Chem.* **2012**, *50*, 2677.
3. Bhatt, S.; Pulpytel, J.; Ceccone, G.; Lisboa, P.; Rossi, F.; Kumar, V.; Arefi-Khonsari, F. *Langmuir* **2011**, *27*, 14570.
4. Hucknall, A.; Rangarajan, S.; Chilkoti, A. *Adv. Mater.* **2009**, *21*, 2441.
5. Page, K.; Wilson, M.; Parkin, I. P. *J. Mater. Chem.* **2009**, *19*, 3819.
6. Kane, R. S.; Deschatelets, P.; Whitesides, G. M. *Langmuir* **2003**, *19*, 2388.
7. Ma, H.; Wells, M.; Beebe, T. P.; Chilkoti, A. *Adv. Funct. Mater.* **2006**, *16*, 640.
8. Banerjee, I.; Pangule, R. C.; Kane, R. S. *Adv. Mater.* **2011**, *23*, 690.
9. Krishnan, S.; Kwark, Y. J.; Ober, C. K. *Chem. Rec.* **2004**, *4*, 315.
10. Krishnan, S.; Wang, N.; Ober, C. K.; Finlay, J. A.; Callow, M. E.; Callow, J. A.; Hexemer, A.; Sohn, K. E.; Kramer, E. J.; Fischer, D. A. *Biomacromolecules* **2006**, *7*, 1449.
11. Holm, E. R.; Kavanagh, C. J.; Meyer, A. E.; Wiebe, D.; Nedved, B. T.; Wendt, D.; Smith, C. M.; Hadfield, M. G.; Swain, G.; Wood, C. D.; Truby, K.; Stein, J.; Montemarano, J. *Biofouling* **2006**, *22*, 233.
12. Jiang, S.; Cao, Z. *Adv. Mater.* **2010**, *22*, 920.
13. Luzon, M.; Boyer, C.; Peinado, C.; Corrales, T.; Whittaker, M.; Tao, L.; Davis, T. P. *J. Polym. Sci. Part A: Polym. Chem.* **2010**, *48*, 2783.
14. Chen, S. F.; Jiang, S. Y. *Adv. Mater.* **2008**, *20*, 335.
15. Chen, Y.; Thayumanavan, S. *Langmuir* **2009**, *25*, 13795.
16. Mrksich, M. *Chem. Soc. Rev.* **2000**, *29*, 267.
17. Craig J. Weinman, N. G. S. K. *Soft Matter* **2010**, *6*, 3237.
18. Krishnan, S.; Weinman, C. J.; Ober, C. K. *J. Mater. Chem.* **2008**, *18*, 3405.
19. Klein, E.; Kerth, P.; Lebeau, L. *Biomaterials* **2008**, *29*, 204.
20. Finlay, J. A.; Krishnan, S.; Callow, M. E.; Callow, J. A.; Dong, R.; Asgill, N.; Wong, K.; Kramer, E. J.; Ober, C. K. *Langmuir* **2008**, *24*, 503.
21. Martinelli, E.; Agostini, S.; Galli, G.; Chiellini, E.; Glisenti, A.; Pettitt, M. E.; Callow, M. E.; Callow, J. A.; Graf, K.; Bartels, F. W. *Langmuir* **2008**, *24*, 13138.
22. Gudipati, C. S.; Finlay, J. A.; Callow, J. A.; Callow, M. E.; Wooley, K. L. *Langmuir* **2005**, *21*, 3044.
23. Zhao, Z.; Ni, H.; Han, Z.; Jiang, T.; Xu, Y.; Lu, X.; Ye, P. *ACS Appl. Mater. Interfaces* **2013**, *5*, 7808.
24. Martinelli, E.; Menghetti, S.; Galli, G.; Glisenti, A.; Krishnan, S.; Paik, M. Y.; Ober, C. K.; Smilgies, D. M.; Fischer, D. A. *J. Polym. Sci. Part A: Polym. Chem.* **2009**, *47*, 267.
25. Hu, Z. K.; Chen, L.; Betts, D. E.; Pandya, A.; Hillmyer, M. A.; DeSimone, J. M. *J. Am. Chem. Soc.* **2008**, *130*, 14244.
26. Wu, L.; Jasinski, J.; Krishnan, S. *J. Appl. Polym. Sci.* **2012**, *124*, 2154.
27. Thanawala, S. K.; Chaudhury, M. K. *Langmuir* **2000**, *16*, 1256.
28. Koberstein, J. T. *J. Polym. Sci. Part B: Polym. Phys.* **2004**, *42*, 2942.
29. Krishnan, S.; Ward, R. J.; Hexemer, A.; Sohn, K. E.; Lee, K. L.; Angert, E. R.; Fischer, D. A.; Kramer, E. J.; Ober, C. K. *Langmuir* **2006**, *22*, 11255.
30. Krishnan, S.; Paik, M. Y.; Ober, C. K.; Martinelli, E.; Galli, G.; Sohn, K. E.; Kramer, E. J.; Fischer, D. A. *Macromolecules* **2010**, *43*, 4733.
31. Colak, S.; Tew, G. N. *Biomacromolecules* **2012**, *13*, 1233.
32. Sundaram, H. S.; Cho, Y. J.; Dimitriou, M. D.; Finlay, J. A.; Cone, G.; Williams, S.; Handlin, D.; Gatto, J.; Callow, M. E.; Callow, J. A.; Kramer, E. J.; Obert, C. K. *ACS Appl. Mater. Interfaces* **2011**, *3*, 3366.
33. Wang, Q.; Zhang, Q.; Zhan, X.; Chen, F. *J. Polym. Sci. Part A: Polym. Chem.* **2010**, *48*, 2584.
34. Sugihara, S.; Kanaoka, S.; Aoshima, S. *Macromolecules* **2004**, *37*, 1711.
35. Kyerematen, S. O.; Amado, E.; Kressler, J. *Eur. Polym. J.* **2007**, *43*, 3380.
36. Thang, S. H.; Chong, Y. K.; Mayadunne, R.; Moad, G.; Rizzardo, E. *Tetrahedron Lett.* **1999**, *40*, 2435.
37. Zhang, G.; Zhang, Q.; Zhan, X. In **2013** AIChE Annual Meeting, San Francisco, United States, Nov 3–8, 2013.
38. Owens, D. K.; Wendt, R. C. *J. Appl. Polym. Sci.* **1969**, *13*, 1741.
39. Kaelble, D. H. *J. Adhes.* **1970**, *2*, 66.
40. Mellon, V.; Rinaldi, D.; Bourgeat-Lami, E.; D'Agosto, F. *Macromolecules* **2005**, *38*, 1591.
41. Liu, S.; Hermanson, K. D.; Kaler, E. W. *Macromolecules* **2006**, *39*, 4345.

42. Skrabania, K.; Berlepsch, H. V.; Boüttcher, C.; Laschewsky, A. *Macromolecules* **2009**, *43*, 271.

43. Fowkes, F. M. *Ind. Eng. Chem.* **1964**, *56*, 40.

44. Della Volpe, C.; Maniglio, D.; Siboni, S.; Morra, M. *J. Adhes. Sci. Technol.* **2003**, *17*, 1477.

45. Krishnan, S.; Ayothi, R.; Hexemer, A.; Finlay, J. A.; Sohn, K. E.; Perry, R.; Ober, C. K.; Kramer, E. J.; Callow, M. E.; Callow, J. A.; Fischer, D. A. *Langmuir* **2006**, *22*, 5075.

46. Nishino, T.; Urushihara, Y.; Meguro, M.; Nakamae, K. *J. Colloid Interface Sci.* **2005**, *283*, 533.

47. Tsibouklis, J.; Graham, P.; Eaton, P. J.; Smith, J. R.; Nevell, T. G.; Smart, J. D.; Ewen, R. *J. Macromolecules* **2000**, *33*, 8460.

48. Al-Hussein, M.; Séréro, Y.; Konovalov, O.; Mourran, A.; Möller, M.; de Jeu, W. H. *Macromolecules* **2005**, *38*, 9610.

49. Ostuni, E.; Yan, L.; Whitesides, G. M. *Colloids Surf. B: Biointerfaces* **1999**, *15*, 3.

50. Li, L.; Chen, S.; Zheng, J.; Ratner, B. D.; Jiang, S. *J. Phys. Chem. B* **2005**, *109*, 2934.

51. Herrwerth, S.; Eck, W.; Reinhardt, S.; Grunze, M. *J. Am. Chem. Soc.* **2003**, *125*, 9359.

52. Colak, S.; Tew, G. N. *Langmuir* **2011**, *28*, 666.

53. Wertz, C. F.; Santore, M. M. *Langmuir* **2001**, *17*, 3006.

54. Baxamusa, S. H.; Gleason, K. K. *Adv. Funct. Mater.* **2009**, *19*, 3489.